Share Your Innovations through JACS Directory

Journal of Nanoscience and Technology

Visit Journal at http://www.jacsdirectory.com/jnst

ISSN: 2455-0191

Effect of Annealing Temperature on Hydrogen Gas Sensitivity of Nanocrystalline SnO_2 Thin Films

S.V. Jagtap[1], A.S. Tale[1], S.D. Thakare[1], M.J. Pawar[2,*]

[1]*Department of Physics, RDIK College, Badnera Rly. Amravati – 444 701, Maharashtra, India.*
[2]*Laboratory of Materials Synthesis, Department of Chemistry, ACS College, Kiran Nagar, Amravati – 444 701, Maharashtra, India.*

ARTICLEDETAILS

Article history:
Received 22 May 2019
Accepted 06 June 2019
Available online 13 June 2019

Keywords:
Sol-Gel Method
Nanocrystalline SnO_2
Gas Sensor

ABSTRACT

Thin films of pure nanocrystalline SnO_2 are deposited using sol–gel technique bare Si (100) substrates at different ageing time and annealing temperatures. The structural and morphological properties of these films are investigated using XRD and TEM techniques. The sensitivity of these films was tested to H_2 gas. A SnO_2 thin film aged for 7 h and annealed at 450 °C shows very high responses to H_2 and excellent selectivity for H_2 gas at a low operating temperature of 50 °C. The response and recovery time of SnO_2 thin films is discussed.

1. Introduction

SnO_2 thin films were extensively studied in the past for their applications as resistors, heat mirrors and electrodes for solar cells based on amorphous hydrogenated silicon [1, 2]. Tin oxide was also investigated as a material for optoelectronic devices [3, 4]. This oxide material has high reactivity towards reducing gases at relatively low operating temperature, easy adsorption of oxygen on its surface because of its natural non-stoichiometry, stable rutile phase and many more desirable attributes such as cheapness and simplicity [5].

The range of application of these types of gas sensors is limited by their poor selectivity, sensitivity and response time. In order to enhance the sensing properties of SnO_2 films, various methods have been adopted such as reduction of grain size, addition of catalysts/promoters and filters, addition of dopants and using mixed metal oxides [6–9]. Most of the commercial and industrial applications require the gas sensors to be operated at lower temperatures (especially at room temperature) to avoid the instability in the nano-crystallite size and hence to increase the robustness and life of sensors [10]. In spite of this, very few attempts [11, 12] have been made to develop nano-crystalline SnO_2 sensors operating at low temperature.

Hydrogen gas is a kind of more efficient and cleaner source of energy which has been used in chemical industries, automobiles, aircraft, fuel cell technologies, alternative fuels etc. [13, 14]. H_2 gas is colorless, odorless, highly volatile, and inflammable and causes explosion when brought in contact with air. Therefore, its detection at room temperature (RT) is very important for chemical industries and environmental applications. RT H_2 gas sensor also attracts much attention in other fields because of their particularly low power consumption [15], the ability to be used safely in flammable environments [16], and long lifetime [17].

This paper focuses on the preparation and fabrication of functional nanocrystalline SnO_2 thin films and performance of H_2 gas sensors at RT for different gas concentrations. The main goal of this study is to effect of annealing temperature on H_2 sensitivity of nanocrystalline SnO_2 thin films deposited on bare Si (100) substrates, to reduce the response time and increase the stability of thin film sensor.

2. Experimental Methods

Nanocrystalline SnO_2 thin films were grown on p-type (100) silicon wafer (10 mm x 10 mm) using sol–gel spin coating method [18, 19]. 0.2 M tin (II) acetate (Sigma Aldrich ≥ 99.9%) was dissolved via 70 mL of pure isopropanol and placed in the covered flasks. The resultant sol solutions in closed flasks were stirred on the magnetic stirrers for 4 h and kept at 70 °C for 7 h and 10 h, respectively. Moreover, glycerin was added to a volume ratio of 1:10 in order to eliminate cracks [20]. The process of preparing the sol solutions was separately completed at room temperature for the remainder of the 24 h. Thereafter, the sol solutions were spin-coated on Silicon wafer (100) substrates at a rotation speed of 4000 rpm for 30 s. The as deposited films were oven-dried at 100°C for 10 min, to obtain high thickness, spin coating and drying operations were repeated multiple times for all samples at different aging heat times. The crystallization of all SnO_2 samples was achieved by annealing at 400 and 450 °C in air ambient for 3 h.

The crystal structures were investigated by X-ray diffractometer (Model Miniflex, Rigaku)) using Cu $K\alpha$ radiation, angle step size of 0.02°, and count time of 1.0 second per step. The microstructures of the thin film samples were characterized by high-resolution transmission electron microscopy (HRTEM; Philips Tecnai F20 G2). X-ray photoelectron spectroscopy (XPS; PHI 5000 VersaProbe) analysis was used to determine the chemical binding status of constituent elements of SnO_2 thin films.

H_2 gas-sensing properties of SnO_2 thin film sensors was measured in terms of the percent sensitivity (S%). The gas sensing experiment was done in a chamber through which air or H_2 gas was allowed to flow at the rate of 250 mLmin^{-1}. The electrical response of the SnO_2 thin film sensors was measured with an automatic test system, controlled by a personal computer. The electrical resistance in air (R_a) and in presence of H_2 gas (R_g) and the percent sensitivity (equation I) of the coatings were measured at room temperature and at 50 °C using a digital multimeter and a constant voltage/current source. A thin layer of Au (~50 nm) was deposited on the SnO_2 layers by vacuum thermal evaporation. Two planar Au electrodes were fabricated on the surface of SnO_2 thin films. The SnO_2 thin films were heated by a heater and a thermocouple was placed on the film surface to measure the temperature. Percent sensitivities (S%) were obtained using the following equation:

$$S\% = \frac{R_a - R_g}{R_a} \times 100 \quad (1)$$

*Corresponding Author:pawarmahendrasingh22@gmail.com(M.J. Pawar)

https://doi.org/10.30799/jnst.264.19050416

3. Results and Discussion

The XRD patterns of SnO_2 thin films annealed at 400 and 450 °C are depicted in Figs. 1 and 2. Figs. 1a and b are for SnO_2 thin films annealed at 400 °C and Figs. 2a and b are for SnO_2 thin films annealed at 450 °C. The peaks correspond to tetragonal rutile structure of SnO_2 (JCPDS card No. 041-1445) [21, 22]. While the peaks in Figs. 2a and b become sharper and stronger as the annealing temperature is increased raised to 450 °C. This is due to the annealing temperature which enhanced the crystallization of films, and therefore increased crystallite size, and reduced defects [22, 23]. The SnO_2 (110) plane was the dominant crystallographic orientation in the SnO_2 samples annealed at both 400 and 450 °C. The average crystallite size (D) of nanocrystalline SnO_2 thin films was calculated using the SnO_2 (110) diffraction peak by Debye-Sherrer formula [20]. It can be seen that the crystallite sizes increase after addition of glycerin as shown in Table 1.

Table 1 Crystallite size of SnO_2 thin films obtained under different conditions

Samples	Aging heat times at (70 °C)	Annealing temp. (°C)	Crystallite size (nm)	Specific surface area (m^2/g)	Lattice constants (a, b, c) [a = b ≠ c] [± 0.003]
SO-1(4)	7 h	400	22.27	45.4	a = b = 4.996 and c = 3.577
SO-2(4)	10 h	400	31.90	42.7	a = b = 4.998 and c = 3.576
SO-1(45)	7 h	450	12.19	56.2	a = b = 4.989 and c = 3.573
SO-2(45)	10 h	450	32.72	41.9	a = b = 4.999 and c = 3.579

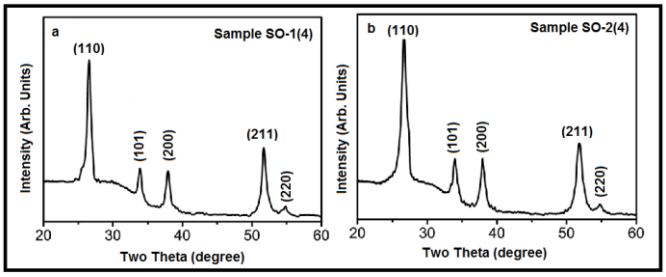

Fig. 1 XRD patterns of the SnO_2 thin films annealed at 400 °C

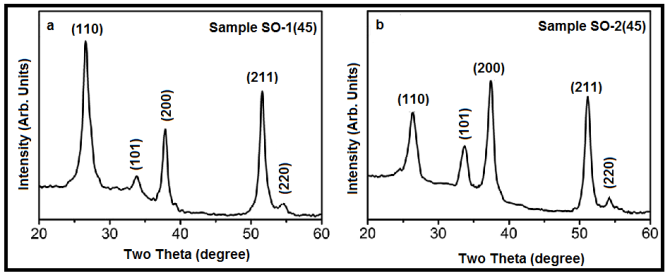

Fig. 2 XRD patterns of the SnO_2 thin films annealed at 450 °C

The microstructures of SnO_2 thin films were further characterized through TEM. Fig. 3(a) shows a low-magnification, cross-sectional TEM image of the SnO_2 thin film which is composed of distinct columnar grains and has a thickness of approximately 120 nm. The film is dense and does not have any visible pores. The top region of the film is smooth. Fig. 3(b) depicts the energy-dispersive X-ray spectroscopy (EDS) spectra of the film, confirming that Sn and O are the major elements in the film's composition.

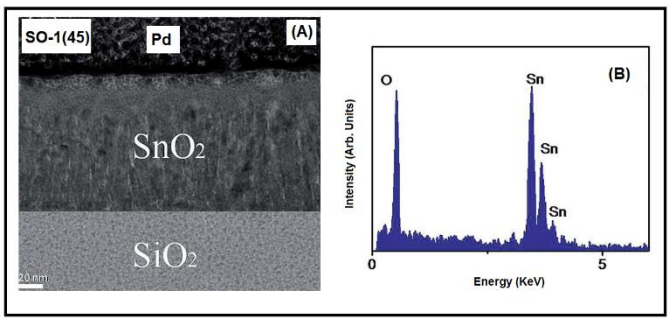

Fig. 3 TEM analysis of SnO_2 thin film (a) low-magnification TEM image of the film (b) EDS spectra of Sn, and O elements taken from the film

Fig. 4 show a symmetric Sn $3d_{5/2}$ peak centered at approximately 486 eV and a Sn $3d_{3/2}$ peak centered at approximately 495 eV; no signal from the metallic Sn was observed. The analysis of XPS narrow scans of the Sn 3d core-level doublet indicated that the Sn^{4+} valence state existed in the form of SnO_2 [24].

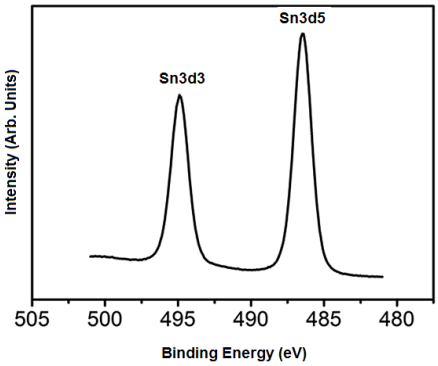

Fig. 4 XPS narrow scans of Sn 3d core level doublet of the SnO_2 thin films annealed at 450 °C

The Figs. 5 and 6 shows the response for different SnO_2 thin film samples as a function of H_2 gas concentration at RT and 50 °C respectively. The response increases linearly as concentration of H_2 gas increased from 100 to 1000 ppm. From Fig. 5, one can see that, the slope for both the SO-1(40) and SO-2(40) samples increased with concentration which is due to interaction of oxygen species and adsorbed H_2 gas on the surface of thin films. For the sample SO-1(40), initially the sensitivity is found to be increased and suddenly drops at about 800 ppm of H_2 gas. This is because, with a small concentration of gas, exposed on a fixed surface area of a sample, there was a lower coverage of H_2 molecules on the surface and hence less surface reaction occurred. An increase in H_2 concentration increases the surface reaction due to a larger surface coverage. Beyond a 750 ppm of H_2 gas concentration, the increase in surface reaction will be gradual, where the saturation point on the coverage of molecules was reached and sensitivity falls.

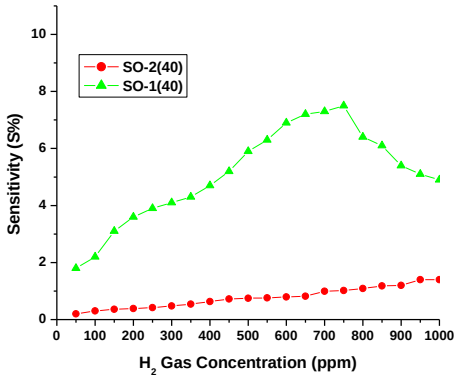

Fig. 5 Sensitivity (%) vs. H_2 gas concentration (ppm) graph for all samples at RT

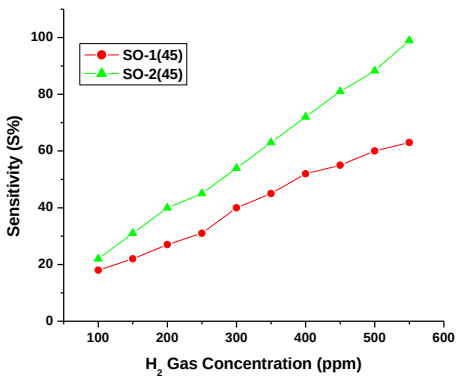

Fig. 6 Sensitivity (%) vs. H_2 gas concentration (ppm) graph for all samples at 50 °C

The transient response characteristics of all the samples at different H_2 gas concentrations are shown at RT and 50 °C in Figs. 7 and 8 respectively. These measurements were performed by injecting H_2 gas into the chamber first and then sensor's resistance was measured in air and in the presence of H_2 gas. All the samples respond rapidly H_2 gas was injected into the chamber at operating temperature 50 °C. At 50 °C, the fast response in case

https://doi.org/10.30799/jnst.264.19050416

Cite this Article as: S.V. Jagtap, A.S. Tale, S.D. Thakare, M.J. Pawar, Effect of annealing temperature on hydrogen gas sensitivity of nanocrystalline SnO_2 thin films, J. Nanosci. Tech. 5(4) (2019) 802–805.

of sample SO-1(45) was attributed to the rapid electron transfer that catalyzes the reaction between the adsorbed gas and the sensor surface. From the results, we have concluded that, for annealing the so prepared SnO_2 thin films, 450 °C is the significant temperature.

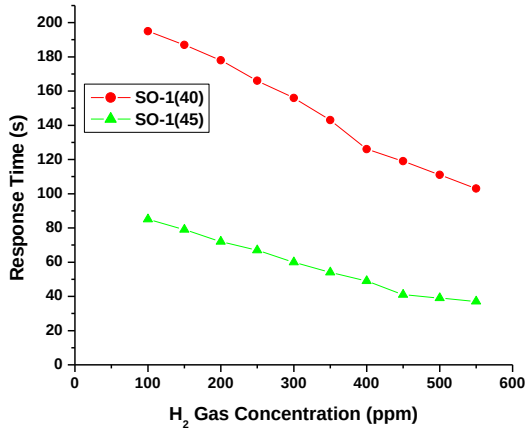

Fig. 7 Response time (s) vs. H_2 gas concentration (ppm) graph for SO-1(40) and SO-1(45) samples at room temperature

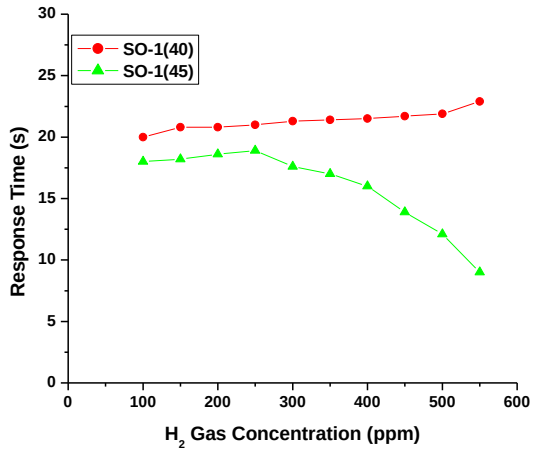

Fig. 8 Response time (s) vs. hydrogen concentration (%) graph for SO-1(40) and SO-1(45) samples at 50 °C

Cross sensitivity of the SO-1(45) sample was tested for carbon monoxide (CO) and ethanol (C_2H_5OH) vapors at operating temperature 50 °C in relation to H_2 gas and the results are presented in Fig. 9. The concentration of gases was varied from 100 to 500 ppm.

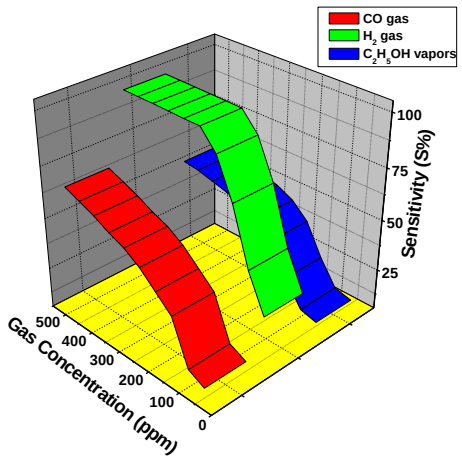

Fig. 9 Cross sensitivity of SO-1(45) sample for different concentrations of CO gas, H_2 gas and ethanol vapors at operating temperature 50 °C

The stability of sensor is the capacity to exhibit constant response over a larger duration. The sensors based on oxide materials have common drawback of decrease in response due to ageing induced effects. Fig. 10 shows the stability graph of the SO-1(45) sensor material and it was measured by repeating the tests for the period of two months from the initial measurement. During the tests, no considerable variations were observed indicating the good stability of the sensor element. The response of the SO-1(45) sensor material sensor to 1% of hydrogen gas concentration at 50°C was measured on 15th, 30th, 45th and 60th days after the first measurement was performed. It was found that after two months, the material performed 98% of its earlier performance and thus confirmed the stability of sensor material for its commercial application.

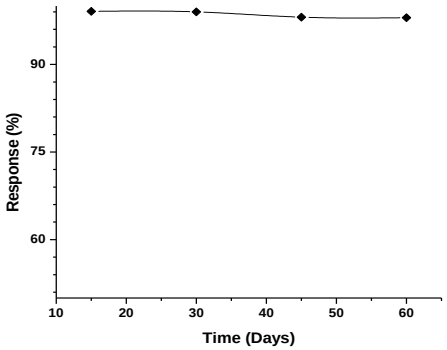

Fig. 10 The stability study for SO-1(45) sample (annealed at 450 °C) at 50 °C for 500 ppm of H_2 gas

The sensing mechanism of nanocrystalline thin films is related to the reduction of the exposure to target gas by the adsorbed oxygen species on the sensor surface. When the surface of nanocrystalline SnO_2 thin films is exposed to ambient air, the oxygen species will be adsorbed (reactions I, II and III). Depending on the operating temperatures, the adsorbed oxygen species get reduced by capturing the electrons from nanocrystalline SnO_2 thin films surface, which increases the depletion region leading to the increase of the resistivity [26]. Depending on the operating temperatures, different oxygen species are formed on adsorption on the sensor surface, which can be described as follows:

$$O_{2(gas)} \rightarrow O_{2(adsorbed)} \quad (2)$$
$$O_{2(adsorbed)} + e^- \rightarrow O_{2^-(adsorbed)} \quad (3)$$
$$O_{2^-(adsorbed)} + e^- \rightarrow 2O^-_{(adsorbed)} \quad (4)$$

H_2 molecules are dissociated to H atom on the Pd contact, which diffused to the surface of thin films, and reacts very quickly with different adsorbed oxygen species by negative charges [25]. Thereby the electrons captured by the oxygen species will return back to the conduction band of thin film, resulting in an increase of electron concentration in the conduction band so that the resistance of nanocrystalline SnO_2 will reduce. The reactions hydrogen with oxygen species could be explained by using the following chemical reactions (IV, V and VI) [28, 29].

$$2H_2 + O_{2^-(adsorbed)} \rightarrow 2H_2O + e^- \quad (5)$$
$$2H_2 + 2O^-_{(adsorbed)} \rightarrow 2H_2O + 2e^- \quad (6)$$
$$4H + O_{2^-(adsorbed)} \rightarrow 2H_2O + e^- \quad (7)$$

The sensitivity of H_2 gas sensor will reduce when the nanocrystalline SnO_2 thin films are exposed to air ambient again, where the air ambient inputs to the gas chamber containing oxygen species. Thereafter, the air oxygen will react with the chemisorbed H_2 on the surface of nanocrystalline SnO_2 thin films. Hence, the resistance of the nanocrystalline SnO_2 thin films goes back to its initial value [25].

4. Conclusion

The response and selectivity of the SnO_2 based gas thin film sensors for H_2 gas have been improved significantly by annealing the material at 400 °C and 450 °C. It has been reported that the annealing temperature not only modifies the surface morphology but also lowers the operating temperature with quick response even at the 100 ppm of H_2 gas.

References

[1] K.L. Chopra, S. Major, D.K. Pandya, Transparent conductors: a status review, Thin Solid Films 102 (1983) 1-46.
[2] R. Banerjee, D. Das, Properties of tin oxide films prepared by reactive electron beam evaporation, Thin Solid Films 149 (1987) 291-301.
[3] C. Tatsuyama, S. Ichimura, Electrical and optical properties of GaSe-SnO, Jpn. J. Appl. Phys. 15 (1976) 843-848.
[4] A. Aoki, H. Sasakura, Tin oxide thin film transistor, Jpn. J. Appl. Phys. 9 (1970) 582.
[5] G. Sberveglieri, C. Baratto, E. Comini, G. Faglia, P. Nelli, L. Dori, Recent progress on gas sensors based on semiconducting thin films, Proc. IEEE 1 (1999) 65–72.
[6] M.J. Madou, S.R. Morrison, Chemical sensing with solid state devices, Academic Press, NY, USA, 1989, p.491.

https://doi.org/10.30799/jnst.264.19050416

[7] C. Xu, J. Tamaki, N. Miura, N. Yamazoe, Grain size effects on gas sensitivity of porous SnO_2 based elements, Sens. Actuators B 3 (1991) 147–155.
[8] G. Martinelli, M.C. Caotta, Thick-film gas sensors, Sens. Actuators B 23 (1995) 157–161.
[9] N. Yamazoe, New approaches for improving semiconductor gas sensors, Sens. Actuators B 5 (1991) 7–19.
[10] S. Shukla, L. Ludwig, C. Parrish, S. Seal, Inverse-catalyst-effect observed for nanocrystalline-doped tin oxide sensor at lower operating temperatures, Sens. Actuators B 104 (2005) 223–231.
[11] M. Penza, C. Martucci, G. Cassano, NOx gas sensing characteristics of WO_3 thin films activated by noble metals (Pd, Pt, Au) layers, Sens. Actuators B 5(1) (1998) 52–59.
[12] W. Goepel, K.D. Schierbaum, SnO_2 sensor current status and future prospects, Sens. Actuators B 77 (1995) 1–12.
[13] S.Y. Chiu, H.W. Huang, K.C. Liang, K.P. Liua, J.H. Tsaib, W.S. Loura, Comprehensive investigation on planar type of pd-GaN hydrogen sensors, Int. J. Hyd. Energy 34(13) (2009) 5604–5615.
[14] W.J. Butter, M.B. Post, R. Burgess, C. RivkinInt, C. Rivkin, An overview of hydrogen safety sensors and requirements, Int. J. Hyd. Energy 36(3) (2011) 2462–2470.
[15] S.J. Peartron, F. Ren, Y.L. Wang, B.H. Chu, K.H. Chen, Progress, recent advances in wide band gap semiconductor biological and gas sensors, Mater. Sci. 55(1) (2010) 1–59.
[16] T. Hubert, L. Boon-black, U. Banach, Hydrogen sensors- A review, Sens. Actuators B 157(2) (2011) 329–352.
[17] S.T. Hung, C.J. Chang, C.H. Hsu, BHChCF Lo, SnO_2 functionalized AlGan/GaN high electron mobility transistor for hydrogen sensing applications, Int. J. Hydr. Energy 37(18) (2012) 13783–13788.
[18] J. Jeng, The influence of annealing atmosphere on the material properties of sol-gel derived SnO_2: Sb films before and after annealing, Appl. Surf. Sci. 258 (2012) 5981–5986.
[19] C.D. Feng, Y. Shimizu, M. Egashira, Effect of gas diffusion process on sensing properties of SnO_2 thin film sensors in a SiO_2/SnO_2 layer-built structure fabricated by sol-gel process, J. Electrochem. Soc. 141(1) (1994) 220–225.
[20] I.H. Kadhim, H.A. Hassan, Effects of glycerin volume ratios and annealing temperature on the characteristics of nanocrystalline tin dioxide thin films, Mater. Sci. Mater: Electron. 26 (2015) 1–10.
[21] M. Aziz, S. Abbas, W. Baharom, Size-controlled synthesis of SnO_2 nanoparticles by sol-gel method, Mater. Lett. 91 (2013) 31–34.
[22] Y. Li, W. Yin, R. Deng, R. Chen, J. Chen, et al., Realizing a SnO_2-based ultraviolet light-emitting diode via breaking the dipole-forbidden rule, NPG Asia Mater. 4 (2012) e30–e36.
[23] C. Ke, W. Zhu, J.S. Pun, Z. Yang, Annealing temperature dependent oxygen vacancy behavior in SnO_2 thin films fabricated by pulsed laser deposition, Curr. Appl. Phys. 11(3) (2011) S306–S309.
[24] Y.C. Liang, H. Zhong, Self-catalytic crystal growth, formation mechanism, and optical properties of indium tin oxide nanostructures, Nanoscale Res. Lett. 8 (2013) 358–368.
[25] Q.N. Abdullah, F.K. Yam, J.J. Hassan, C.W. Chin, High performance room temperature GaN-nanowires hydrogen gas sensor fabricated by chemical vapour deposition (CVD) technique, Int. J. Hyd. Energy 38 (2013) 14085–14101.
[26] M.L. Lu, T.M. Weng, J.Y. Chen, Y.F. Chen, Ultrahigh-gain single SnO_2 nanowire photodetectors made with ferromagnetic nickel electrodes, NPG Asia Mater. 4 (2012) e26–e31.
[27] K.K. Khun, A. Mahajan, R.K. Bedi, SnO_2 thick films for room temperature gas sensing applications, J. Appl. Phys. 106 (2009) 124509–124514.
[28] S.S. Kim, J.Y. Park, S.W. Choi, H.S. Kim, H.G. Na, Room temperature sensing properties of networked GaN nanowire sensors to hydrogen enhanced by the Ga_2Pd_5 nanodot functionalization. Int. J. Hyd. Energy 36(3) (2011) 2313–2319.
[29] J.J. Hassan, M.A. Mahdi, C.W. Chin, H. Abu-Hassan, Room temperature hydrogen gas sensor based on ZnO nanorod arrays grown on a SiO_2/Si substrate via a microwave-assisted chemical solution method, J. Alloys Compd. 546 (2013) 107–111.

https://doi.org/10.30799/jnst.264.19050416

Cite this Article as: S.V. Jagtap, A.S. Tale, S.D. Thakare, M.J. Pawar, Effect of annealing temperature on hydrogen gas sensitivity of nanocrystalline SnO_2 thin films, J. Nanosci. Tech. 5(4) (2019) 802–805.